Revised Submission to the AIAA Journal of Guidance, Control, & Dynamics

Fuel Optimization for Constrained Rotation of Spacecraft Formations

Randal W. Beard* Timothy W. McLain†

Brigham Young University, Provo, Utah 84602

Fred Y. Hadaegh‡

Jet Propulsion Laboratory, California Institute of Technology,

Pasadena, California 91101

Abstract

This paper considers the problem of reorienting a constellation of spacecraft such that the fuel distributed across the constellation is both conserved and expended uniformly. Results are derived for constellations with an arbitrary number of spacecraft, assuming that

*Assistant Professor, Department of Electrical and Computer Engineering. Member AIAA.

†Assistant Professor, Department of Mechanical Engineering. Member AIAA.

‡Senior Research Scientist and Technical Supervisor, Automation and Control Section. Associate Fellow of AIAA.

the constellation is in free space, that the spacecraft mass is time-invariant, and that the thrusters can produce thrust in any direction. An open-loop control algorithm is derived by minimizing a cost function that trades off total fuel minimization and fuel equalization. The associated optimization problem is shown to be amenable to standard algorithms. Simulation results using a four-spacecraft constellation are given.

Introduction

Multiple spacecraft formation flying is emerging as an enabling technology for a number of planned NASA missions. An example is the proposed separated spacecraft interferometry missions.[1] Since the life expectancy of a satellite is limited by its fuel, fuel optimization is critically important to formation control algorithms. For various applications of spacecraft formation flying, including interferometry, the formation is required to assume several orientations. In this paper we will consider the problem of rotating a formation from one orientation to another. A key observation is that the inertial point about which the formation rotates determines the amount of fuel consumed by each spacecraft. For example, if the formation rotates about a single spacecraft, then that spacecraft will not consume fuel, while the other spacecraft consume disproportionately large amounts of fuel. The objective of this paper is to evaluate strategies for determining a fuel optimal point of rotation given the current and desired constellation configurations and rotation angles. In evaluating these strategies, two quantities are of primary interest: the total fuel used by the spacecraft in the constellation and the

distribution of fuel usage among the spacecraft in the constellation. Not only is it desirable to minimize the total combined fuel expended by the formation during a maneuver, it is perhaps even more desirable to ensure that no spacecraft is starved of fuel, i.e., it is desirable that all of the spacecraft run out of fuel simultaneously. The reason that it is important to avoid fuel starvation for interferometry missions is because when one spacecraft runs out of fuel the mission must be terminated, even though the remaining spacecraft still have fuel. It turns out that fuel minimization and equalization are competing objectives. The contribution of this paper is to derive open-loop control strategies that explicitly tradeoff these two objectives.

Central to these control strategies is the determination of the point of rotation for the constellation. This paper will explore how to pick a point of rotation such that the fuel distribution at the end of the maneuver is equalized and the total fuel expended by the constellation is as small as possible. This is done by formulating a cost function containing two terms. The first term penalizes the fuel expended during a maneuver. The second term is motivated by the entropy function from information theory which has the property that it is maximized by a uniform probability mass function,[2] thereby penalizing an unequal fuel distribution at the end of the maneuver. The point of rotation for the constellation is obtained by optimizing this cost function. Once the point of rotation is determined, it is fixed for the duration of the constellation rotation and cannot adapt to reflect fuel expenditure that may be different than what was anticipated.

Wang & Hadaegh developed formation flying strategies for tightly controlled satellite constellations using nearest neighbor tracking laws to main-

tain relative position and attitude between spacecraft.[3] Their approach is extended in Ref. 4 to the problem of continuous rotational slews.

The application of space-based formation flying to interferometry is discussed in Ref. 1. DeCou[5] studies passive formation control for geo-centric orbits in the context of interferometry. McInnes[6] uses Lyapunov control functions to maintain a constellation of satellites in a ring formation. Ulybyshev[7] uses an LQ regulator approach for relative formation keeping. Formation initialization has been studied in Ref. 8.

An approach related to Ref. 3 is reported in Ref. 9. The basic idea is to treat the spacecraft constellation as a system of bodies that are fixed relative to each other, and then control the system as a whole.

Preliminary results were originally reported in Ref. 10, where fuel optimization was performed in two dimensions. Similar results are reported in Ref. 11 where the spacecraft are not required to maintain relative positioning throughout the maneuver.

The remainder of this paper is organized as follows. In the first section our notation is defined and the basic assumptions made throughout the paper are stated. In the second section the cost function is defined, and the basic open-loop control algorithm is derived. The third section analyzes the cost function and discusses an optimization algorithm. In the fourth section simulation results using a constellation with four spacecraft are discussed. Finally, the last section gives our conclusions.

Definitions and Assumptions

This section establishes the notation and assumptions that will be used throughout the paper. Assuming that there are N spacecraft in the constellation, define $N+2$ coordinate frames as follows. Let $\mathcal{C}_O$ be the inertial coordinate frame with orthonormal basis vectors $\{\mathbf{i}_O, \mathbf{j}_O, \mathbf{k}_O\}$. Let $\mathcal{C}_R$ be a coordinate frame designated as the "rotation frame," with orthonormal basis vectors $\{\mathbf{i}_R, \mathbf{j}_R, \mathbf{k}_R\}$. The frame $\mathcal{C}_R$ is used to specify the point of rotation of the constellation. With each of the N spacecraft is associated a coordinate frame $\mathcal{C}_\ell$ with associated orthonormal bases $\{\mathbf{i}_\ell, \mathbf{j}_\ell, \mathbf{k}_\ell\}$.

Let $\mathbf{r}_\ell$, and $\mathbf{r}_R$ be the position vectors of coordinate frames $\mathcal{C}_\ell$, and $\mathcal{C}_R$ respectively, in the inertial frame. Also let $\mathbf{r}_{R\ell}$ be defined as the vectors from $\mathcal{C}_R$ to $\mathcal{C}_\ell$. To maintain the constellation formation throughout a rotation maneuver, it is desired that $\mathbf{r}_{R\ell}$ remain constant with respect to the rotation frame $\mathcal{C}_R$. The geometry is shown in Figure 1.

Define M_ℓ to be the mass of the ℓ^{th}spacecraft, and $f_\ell(t)$ to be the fuel mass contained on the ℓ^{th}spacecraft at time t. Furthermore, assume each spacecraft is equipped with an orthogonal set of thrusters capable of producing thrust $\mathbf{T}_\ell$ in any direction. The dynamics for the ℓ^{th}spacecraft are modeled by the following equations:

$$
\begin{aligned}
M_\ell \ddot{\mathbf{r}}_\ell &= \begin{cases} \mathbf{T}_\ell; & f_\ell(t) > 0 \\ \mathbf{0}; & \text{otherwise,} \end{cases} \\
\dot{f}_\ell &= \begin{cases} -\gamma(|T_{a\ell}| + |T_{r\ell}| + |T_{t\ell}|); & f_\ell(t) > 0 \\ 0; & \text{otherwise,} \end{cases}
\end{aligned} \tag{1}
$$

where γ is a proportionality constant, and where $T_{a\ell}$, $T_{r\ell}$ and $T_{t\ell}$ are the axial, radial, and transverse components of $\mathbf{T}_\ell$ expressed in the $\mathcal{C}_\ell$ coordinate frame.

The control objective is to rotate the entire constellation through an angle $\hat{\phi}$ about a unit vector $\mathbf{z}$ which is referenced to the coordinate frame $\mathcal{C}_R$. This rotation can be specified by a unit quaternion $\mathbf{q} = \left(\mathbf{z}^T \sin(\hat{\phi}/2), \cos(\hat{\phi}/2)\right)^T$. Given a rotation quaternion $\mathbf{q}$, the quantities $\mathbf{z}$ and $\hat{\phi}$ can be found by the inverse quaternion formulas given in Ref. 12.

Assumptions

The major assumptions made throughout the paper are listed below. (1) The constellation is in free space. (2) The thrust magnitude of the thrusters for an individual spacecraft is finite, but collectively the thrusters can produce force in any direction. (3) Each spacecraft is a rigid body with mass that is time-invariant. (4) Rotations of the spacecraft are carried out using means other than thrusters (e.g., momentum wheels), therefore rotational motion is not considered when calculating fuel usage. (5) The position $\mathbf{r}_\ell$ of each spacecraft can be determined with respect to the coordinate frame $\mathcal{C}_O$. (6) The thrust magnitude is allowed to range continuously between the saturation limits of the thruster.

Note that these assumptions imply perfect navigation information and perfect thruster performance. Robustness of the derived methods with respect to imperfect navigation information and thrusters has not been studied.

If any of the above assumptions are relaxed, the results of this paper will need to be modified. For example, if the constellation is not in free space,

then orbital dynamics will affect the fuel consumption. If certain thrust directions cannot be produced, then a sequence of maneuvers may be required to accomplish a rotation, thereby requiring a different fuel analysis. If the mass of the fuel is on the order of the mass of the spacecraft, then the analysis in this paper would need to be modified to use the rocket equation. Similarly, rotational dynamics would add an additional level of complexity. Addressing the last two assumptions is necessary to accomplish fixed formation maneuvers in general.

Static Rotations

This section derives an algorithm for picking the location of the rotation point, i.e. $\mathbf{r}_R$, such that given the initial fuel distribution $\{f_1(t_0), \ldots, f_N(t_0)\}$, the final fuel distribution $\{f_1(t_0+t_f), \ldots, f_N(t_0+t_f)\}$ minimizes the following functional:

$$J = \min_{\mathbf{r}_R} \left\{ \sum_{\ell=1}^{N} \left(f_\ell(t_0) - f_\ell(t_0+t_f)\right)^2 + \mu \sum_{\ell=1}^{N} \frac{f_\ell(t_0+t_f)}{\sum_{j=1}^{N} f_j(t_0+t_f)} \log \frac{f_\ell(t_0+t_f)}{\sum_{j=1}^{N} f_j(t_0+t_f)} \right\}. \tag{2}$$

The first term in this functional represents the total amount of fuel expended by the constellation. The second term is motivated by the negative entropy of a probability distribution [2, pp. 12–15], which is minimum for a uniform distribution, i.e., the second term will be minimized when $f_i(t_0+t_f) = f_j(t_0+t_f)$ for all $i, j \in \{1, \ldots, N\}$.

An alternative to entropy is the function

$$\sum_{i=1}^{N}\sum_{j\neq i}^{N}[f_i(t_0+t_f)-f_j(t_0+t_f)]^2\,, \tag{3}$$

which is also minimized when $f_i(t_0+t_f)=f_j(t_0+t_f)$. The use of Equation (3) gives similar results to those reported in this paper. The entropy term was selected because in simulation studies, it equalized the fuel distribution more uniformly.

To minimize Equation (2), we need to express $f_\ell(t_0+t_f)$ in terms of $\mathbf{r}_R$. For a given $\mathbf{r}_R$, $f_\ell(t_0+t_f)$ is found in two steps: first, determine a constellation rotation trajectory within the thrust capability of each spacecraft in the constellation; and second, calculate the fuel consumed by each spacecraft in following the rotation trajectory. The details of these steps are discussed in the next two sections.

Constellation Rotation Trajectory

First note that the rotational acceleration for the constellation is limited by the linear acceleration capability of each spacecraft and by the distance of each spacecraft from the axis specified by $\mathbf{z}$. Since we are considering the rotation of individual spacecraft about a fixed axis in space, the acceleration of each spacecraft is composed of transverse and radial (centripetal) accelerations with respect to the rotation axis: $\mathbf{a}_\ell=\mathbf{a}_{t\ell}+\mathbf{a}_{r\ell}$, where $\mathbf{a}_{t\ell}$ and $\mathbf{a}_{r\ell}$ are the transverse and radial accelerations, respectively.

Let $\mathbf{d}_\ell$ be the shortest vector between the rotation axis $\mathbf{z}$ and the ℓ^{th}spacecraft, and define $\phi(t)$ as the constellation rotation angle. The vector $\mathbf{d}_\ell$ can be found

by using the geometry shown in Figure 2. The projection of $\mathbf{r}_{R\ell}$ onto the $\mathbf{z}$ axis is given by $\mathbf{z}^T\mathbf{r}_{R\ell}$, where $\mathbf{z}$ and $\mathbf{r}_{R\ell}$ are referenced to the same coordinate frame. Therefore, the shortest vector from the $\mathbf{z}$ axis to $\mathcal{C}_\ell$ is

$$\mathbf{d}_\ell = \mathbf{r}_{R\ell} - (\mathbf{z}^T\mathbf{r}_{R\ell})\mathbf{z} = (I - \mathbf{z}\mathbf{z}^T)\mathbf{r}_{R\ell}, \tag{4}$$

where I is the 3×3 identity matrix.

For general rotations $\|\mathbf{a}_{r\ell}\| = \|\mathbf{d}_\ell\|\,\dot{\phi}^2$ and $\|\mathbf{a}_{t\ell}\| = \|\mathbf{d}_\ell\|\,\ddot{\phi}$, therefore it can be seen that the magnitude of the acceleration for each spacecraft is proportional to the distance of the spacecraft from the rotation axis:

$$\|\mathbf{a}_\ell\| = \|\mathbf{d}_\ell\|\,\sqrt{\ddot{\phi}(t)^2 + \dot{\phi}(t)^4}.$$

If we define τ_ℓ as the magnitude of the smallest available maximum thrust in any direction for the ℓ^{th}spacecraft (i.e., spacecraft ℓ can produce a thrust of at least τ_ℓ in any specified direction), then the lowest maximum linear acceleration that each spacecraft is capable of is τ_ℓ/M_ℓ:

$$\|\mathbf{d}_\ell\|\,\sqrt{\ddot{\phi}(t)^2 + \dot{\phi}(t)^4} \leq \frac{\tau_\ell}{M_\ell}.$$

The maximum angular acceleration of the constellation will be maximally constrained by the linear acceleration capability of the spacecraft in the constellation. Specifically, the spacecraft with the largest ratio between the distance from the $\mathbf{z}$ axis ($\|\mathbf{d}_\ell\|$) and its acceleration capability (τ_ℓ/M_ℓ), will limit the angular acceleration of the entire constellation. Denoting the index

of the limiting spacecraft as β gives

$$\beta = \arg \max_{1 \leq \ell \leq N} \frac{M_\ell}{\tau_\ell} \|\mathbf{d}_\ell\| . \tag{5}$$

The angular motion of the entire constellation, given by $\phi(t)$, must be constrained according to the following relation:

$$\sqrt{\ddot{\phi}(t)^2 + \dot{\phi}(t)^4} \leq \frac{\tau_\beta}{M_\beta \|\mathbf{d}_\beta\|}. \tag{6}$$

By constraining the motion in this manner, the required thrust to track whatever trajectory is specified will never exceed the thrust capabilities of any of the spacecraft. Furthermore, this conservative approach leaves some excess thrust capability for rejecting disturbances or responding to tracking errors.

To estimate the amount of fuel spent by each spacecraft during a constellation rotation, a trajectory for the rotation must be determined. The analysis given here assumes that the constellation is rotated via a trajectory corresponding to a bang-off-bang acceleration profile. This thrust profile is optimal [13, pp. 675–710] for a double-integrator plant with actuator saturation. Although linear accelerations during the acceleration and deceleration phases of the trajectory are not constant for each spacecraft (the centripetal component changes with $\dot{\phi}$), the assumption of a bang-off-bang trajectory is a reasonable approach for the constellation rotation problem. The analysis approach taken is not limited to bang-off-bang trajectories. Other trajectories, such as polynomial splines, could be analyzed as well.

Letting $\phi(t)$ be the rotation angle of the constellation about the $\mathbf{z}$ axis at

time t, where t_0 is the starting time for the rotation, the rotation trajectory for the constellation is given by the following equations

$$\ddot{\phi}(t) = \begin{cases} \alpha; & 0 \leq t - t_0 \leq t_w \\ 0; & t_w \leq t - t_0 \leq t_f - t_w \\ -\alpha; & t_f - t_w \leq t - t_0 \leq t_f, \end{cases}$$

$$\dot{\phi}(t) = \begin{cases} \alpha t; & 0 \leq t - t_0 \leq t_w \\ \alpha t_w; & t_w \leq t - t_0 \leq t_f - t_w \\ \alpha(t_f - t); & t_f - t_w \leq t - t_0 \leq t_f, \end{cases} \tag{7}$$

$$\phi(t) = \begin{cases} \frac{1}{2}\alpha t^2; & 0 \leq t - t_0 \leq t_w \\ \alpha[t_w t - \frac{t_w^2}{2}]; & t_w \leq t - t_0 \leq t_f - t_w \\ \alpha[t_w(t_f - t_w) - \frac{(t_f - t)^2}{2}]; & t_f - t_w \leq t - t_0 \leq t_f, \end{cases}$$

where t_w is the width of the thrust pulse.

Notice that the maximum linear acceleration for each of the spacecraft in the constellation occurs at $t - t_0 = t_w$ when $\ddot{\phi}(t)$ and $\dot{\phi}(t)$ are at their maxima simultaneously: $\ddot{\phi}(t_w + t_0) = \alpha$ and $\dot{\phi}(t_w + t_0) = \alpha t_w$.

With the constellation geometry and trajectory type determined, the next step is to formulate an expression that will allow us to solve for the unknown trajectory parameters (α and t_w) given the constellation parameters ($\|\mathbf{d}_\beta\|$, τ_β, and M_β) and the specified trajectory parameters ($\hat{\phi}$ and t_f). This is done by first setting the maximum acceleration of spacecraft β (which is tracking

the bang-off-bang rotation trajectory) to the acceleration bound:

$$\|\mathbf{d}_\beta\| \sqrt{\alpha^2 + (\alpha t_w)^4} = \frac{\tau_\beta}{M_\beta}. \tag{8}$$

Using the fact that $\hat{\phi} = \phi(t_f + t_0) = \alpha t_w(t_f - t_w)$ we can solve for α to obtain

$$\alpha = \frac{\hat{\phi}}{t_w(t_f - t_w)}. \tag{9}$$

By substituting for α in Equation (8) and manipulating the resulting expression, we find that

$$\frac{\hat{\phi}^2}{c^2(1-c)^2} + \frac{\hat{\phi}^4}{(1-c)^4} = \left(\frac{\tau_\beta t_f^2}{\|\mathbf{d}_\beta\| M_\beta}\right)^2 \tag{10}$$

where

$$t_w = ct_f; \qquad 0 < c \leq \tfrac{1}{2}. \tag{11}$$

Further manipulation yields a 6th-order polynomial in c:

$$\Psi(c) = c^6 - 4c^5 + 6c^4 - 4c^3 - \frac{\hat{\phi}^4 + \hat{\phi}^2 - K}{K}c^2 + 2\frac{\hat{\phi}^2}{K}c - \frac{\hat{\phi}^2}{K} = 0 \tag{12}$$

where $K = \left(\frac{\tau_\beta t_f^2}{\|\mathbf{d}_\beta\| M_\beta}\right)^2$. When solving this expression for c, we are interested in the real roots that fall within the range $(0, \frac{1}{2})$, since roots outside this range are physically meaningless. As Figure 3 depicts, solution of Equation (12) results in four scenarios of interest: (1) no roots between 0 and $\frac{1}{2}$; (2) two identical roots between 0 and $\frac{1}{2}$; (3) two different roots between 0 and $\frac{1}{2}$; and

(4) one root between 0 and $\frac{1}{2}$. Case 1 results when the trajectory duration t_f is too short for spacecraft β to accomplish the trajectory given the rotation angle and its acceleration capabilities. Case 2 occurs when the minimum possible trajectory duration that is within the capabilities of spacecraft β is chosen. Case 3 is unusual in that two different values of c are found which result in Equation (8) being satisfied. However, the smaller value of c gives a more fuel-efficient trajectory and therefore is chosen when Case 3 occurs. Case 4 occurs when the acceleration capabilities of the spacecraft are not stressed by the selection of t_f.

In selecting the trajectory duration, two specific conditions are of interest: Case 2 which results in the minimum possible trajectory duration for the formation, and the transition between Cases 3 and 4 where one real root is equal to $\frac{1}{2}$. We will consider the latter condition first.

If t_f is chosen to be sufficiently large, Case 4 results and the desired trajectory is well within the capabilities of the spacecraft. The transition between Case 3 and Case 4 occurs when $t_w = t_f/2$. Letting $t_w = t_f/2$ in Equation (9) and substituting into the acceleration bound in Equation (8) gives

$$\left(\frac{\tau_\beta}{M_\beta \left\|\mathbf{d}_\beta\right\|}\right)^2 = \frac{\hat{\phi}^2}{\left(\frac{t_f}{2}\right)^4} + \frac{\hat{\phi}^4}{\left(\frac{t_f}{2}\right)^4}.$$

Solving for t_f gives

$$t_{f,4} = 2\sqrt{\frac{M_\beta \left\|\mathbf{d}_\beta\right\|}{\tau_\beta}\hat{\phi}\sqrt{1+\hat{\phi}^2}}.$$

When $t_f = t_{f,4}$ the result is Case 3 with one of the roots of Equation (12) being exactly $\frac{1}{2}$ as expected. If $t_f > t_{f,4}$ then there is always a unique solution in the interval $(0, \frac{1}{2})$.

Of greater interest is the minimum possible trajectory duration, $t_{f,min}$, for the spacecraft formation (Case 2). For a given constellation of spacecraft (with predetermined capabilities) and a specified rotation angle $\hat{\phi}$, the selection of trajectory duration t_f determines which of the above cases results. As can be seen from Figure 3, Case 2 occurs when $\Psi(c) = 0$ and $\frac{d\Psi}{dc} = 0$ for the same $c = c_0$: $\frac{d\Psi}{dc}|_{c=c_0} = \Psi(c)|_{c=c_0} = 0$, where

$$\frac{d\Psi}{dc} = 6c^5 - 20c^4 + 24c^3 - 12c^2 - \frac{2(\hat{\phi}^4 + \hat{\phi}^2 - K)}{K}c + 2\frac{\hat{\phi}^2}{K} \tag{13}$$

is determined from Equation (12). By equating the expressions for $\Psi(c)$ and $\frac{d\Psi}{dc}$ the following polynomial expression results:

$$c^6 - 10c^5 + 26c^4 - 28c^3 - \frac{\hat{\phi}^4 + \hat{\phi}^2 - 13K}{K}c^2 + \frac{2(\hat{\phi}^4 + 2\hat{\phi}^2 - K)}{K}c - \frac{3\hat{\phi}^2}{K} = 0, \tag{14}$$

where in this case, $K = \left(\frac{\tau_\beta t_{f,min}^2}{\|\mathbf{d}_\beta\| M_\beta}\right)^2$. This expression can be solved for $c = c_0$ by finding the real root between 0 and $\frac{1}{2}$. Once c_0 is known, the minimum final time $t_{f,min}$ can be calculated by rewriting Equation (10) as

$$t_{f,min} = \left[\left(\frac{\|\mathbf{d}_\beta\| M_\beta}{\tau_\beta}\right)^2 \left(\frac{\hat{\phi}^2}{c_0^2(1-c_0)^2} + \frac{\hat{\phi}^4}{(1-c_0)^4}\right)\right]^{\frac{1}{4}}. \tag{15}$$

Notice that $t_{f,min}$ is dependent on c_0, and that c_0 is dependent on K, and

that K is dependent on $t_{f,min}$. To solve for $t_{f,min}$, Equations (14) and (15) are solved recursively starting with an initial estimate of $t_{f,min} = t_{f,4}$. Convergence to the solution typically requires only several recursions. From the value of c found from the roots of $\Psi(c)$, values for α and t_w can be calculated from Equations (9) and (11) respectively.

In summary, given a specified constellation rotation angle $\hat{\phi}$, trajectory duration $t_f > t_{f,min}$, and the thrust capability τ_β, mass M_β, and distance from the rotation axis $\|\mathbf{d}_\beta\|$ of the limiting spacecraft, the parameters that complete the characterization of the constellation rotation trajectory can be determined: the switching time t_w and the angular acceleration α.

In this development, we treat the trajectory duration, or alternatively the time required for the formation reorientation to be completed, as a parameter to be selected. Intuitively, the trajectory duration also strongly affects the amount of fuel required to complete the maneuver. If fuel minimization is a high priority, the trajectory duration should be selected as large as possible while still meeting the mission objectives.

Fuel Usage

We must now derive an expression that relates the fuel expended by the ℓ^{th}spacecraft to the trajectory of the constellation. The fuel usage for each spacecraft will vary throughout the rotation maneuver and can be calculated for each of the three phases of the trajectory: acceleration, coast, and deceleration.

During the acceleration phase, fuel is expended to accelerate the spacecraft transversely and radially with respect to rotation about the $\mathbf{z}$ axis.

Drawing on Equation (1) the fuel expended by spacecraft ℓ during the acceleration phase can be calculated as follows:

$$\begin{aligned} f_\ell(t_w + t_0) - f_\ell(t_0) &= -\gamma \int_{t_0}^{t_w+t_0} (|T_{a\ell}| + |T_{r\ell}| + |T_{t\ell}|)dt \\ &= -\gamma M_\ell \|\mathbf{d}_\ell\| \int_{t_0}^{t_w+t_0} (\alpha + \alpha^2(t - t_0)^2)dt \\ &= -\gamma M_\ell \|\mathbf{d}_\ell\| \alpha \left(t_w + \alpha \frac{t_w^3}{3} \right) \end{aligned}$$

During the coast phase of the trajectory ($t_w < t - t_0 \leq t_f - t_w$), the spacecraft will need to thrust to provide the centripetal acceleration required to track the arc traced out by the constellation. The fuel required to accomplish this is given by

$$\begin{aligned} f_\ell(t_f - t_w + t_0) - f_\ell(t_w + t_0) &= -\gamma \int_{t_w+t_0}^{t_f-t_w+t_0} (|T_{a\ell}| + |T_{r\ell}| + |T_{t\ell}|)dt \\ &= -\gamma M_\ell \|\mathbf{d}_\ell\| \alpha^2 t_w^2 \int_{t_w+t_0}^{t_f-t_w+t_0} dt \\ &= -\gamma M_\ell \|\mathbf{d}_\ell\| \alpha^2 t_w^2 (t_f - 2t_w). \end{aligned}$$

During the deceleration phase, fuel is expended to bring the spacecraft to a stop and to keep the spacecraft rotating about the $\mathbf{z}$ axis. Fuel usage is

calculated in a manner similar to the previous phases:

$$\begin{aligned} f_\ell(t_f + t_0) - f_\ell(t_f - t_w + t_0) &= -\gamma \int_{t_f - t_w + t_0}^{t_f + t_0} (|T_{a\ell}| + |T_{r\ell}| + |T_{t\ell}|) dt \\ &= -\gamma M_\ell \|\mathbf{d}_\ell\| \int_{t_f - t_w + t_0}^{t_f + t_0} \left(\alpha + \alpha^2 (t_f - t + t_0)^2\right) dt \\ &= -\gamma M_\ell \|\mathbf{d}_\ell\| \alpha \left(t_w + \alpha \frac{t_w^3}{3}\right). \end{aligned}$$

The total fuel consumed by the ℓ^{th}spacecraft during the rotation of the constellation is given by the sum of the fuel consumed during each of the three phases:

$$f_\ell(t_f + t_0) - f_\ell(t_0) = -\gamma M_\ell \|\mathbf{d}_\ell\| \alpha \left(2t_w + \alpha^2 t_w^2 t_f - \frac{4}{3}\alpha t_w^3\right). \tag{16}$$

The Optimal Point of Rotation

The results of the previous section can be summarized by the following algorithm for computing the cost function J in Equation (2).

Algorithm 1

Input: $\mathbf{r}_R$, $\mathbf{q}$, t_f, μ, *and* $\{\tau_\ell, M_\ell, \mathbf{r}_\ell(t_0), f_\ell(t_0)\}_{\ell=1}^N$,

Compute:

1. $\mathbf{z}$, $\hat{\phi}$,
2. $\mathbf{r}_{R\ell}(t_0) = \mathbf{r}_\ell(t_0) - \mathbf{r}_R$, $\ell = 1, \ldots, N$,
3. $\mathbf{d}_\ell(t_0)$, $\ell = 1, \ldots, N$ *from Equation* (4),
4. β *from Equation* (5),
5. c *from Equation* (12),

6. t_w *from Equation* (11),
7. α *from Equation* (9),
8. $f_\ell(t_f + t_0)$ *from Equation* (16).

Output: J *from Equation* (2).

It is evident from Equation (2) and the algorithm listed above, that J is a complicated function of $\mathbf{r}_R$. It is natural to wonder about the difficulty of optimizing J. The next section contains a mathematical analysis of the cost function, and is followed by our recommendations for an algorithm that optimizes J as a function of $\mathbf{r}_R$.

Analysis of the Cost Function

The objective of this section is to analyze the nature of J. Figure 4 shows four contour plots of J, projected onto a plane perpendicular to $\mathbf{z}$, as a function of $\mathbf{r}_R$ for the parameters listed in Table 1. The 'X's in the figure represent the location of the spacecraft. The 'O' represents the center of inverse fuel mass, defined as

$$\mathbf{r}_R^{(0)} = \frac{\sum_{\ell=1}^{N} \mathbf{r}_\ell(t_0)/f_\ell(t_0)}{\sum_{j=1}^{N} 1/f_j(t_0)}. \tag{17}$$

Intuitively, $\mathbf{r}_R^{(0)}$ will be close to spacecraft that are low on fuel. Figure 4 (a) shows J when the initial fuel is equally distributed among the spacecraft, and where fuel equalization is emphasized. Figure 4 (b) shows J when fuel minimization is emphasized. When $\mu = 0$, the initial fuel distribution is not relevant. Figures 4 (c) and (d) are for medium values of μ ($\mu = 100$). Figure 4 (c) shows J when one spacecraft is almost depleted of fuel. In that

case, the optimal $\mathbf{r}_R$ is located close to the spacecraft that is depleted of fuel. Figure 4 (d) shows J when two spacecraft are almost depleted of fuel. In that case, the "optimal" $\mathbf{r}_R$ is centered between the spacecraft that are low on fuel.

Figure 4 shows cusps in the contour plot J that appear to be aligned along certain lines. These cusps suggest that the gradient of J is discontinuous along these lines. Also, the smoothness of the contours away from these lines suggest that J is continuously differentiable in most of $\mathbb{R}^3$. These observations will be made precise in the following Lemmas. The apparent regions come from the partitioning due to Equation (5). Let $\mathcal{D}_j$ be the region in $\mathbb{R}^3$ that is farther from the j^{th} spacecraft than from any other spacecraft (weighted by M_j/τ_j). These regions can be defined explicitly as follows. Let

$$\begin{aligned}\mathcal{D}_j &= \{\mathbf{x} \in \mathbb{R}^3 \ : \ j = \arg\max_{1\le\ell\le N} \frac{M_\ell}{\tau_\ell} \|\mathbf{d}_\ell - \mathbf{x}\|\} \\ &= \cap_{i\neq j}\{\mathbf{x} \in \mathbb{R}^3 \ : \ \frac{M_j}{\tau_j} \|\mathbf{d}_j - \mathbf{x}\| > \frac{M_i}{\tau_i} \|\mathbf{d}_i - \mathbf{x}\|\}.\end{aligned}$$

Define $\bar{\mathcal{D}}_j$ as the closure of $\mathcal{D}_j$, i.e.,

$$\bar{\mathcal{D}}_j = \cap_{i\neq j}\{\mathbf{x} \in \mathbb{R}^3 \ : \ \frac{M_j}{\tau_j} \|\mathbf{d}_j - \mathbf{x}\| \ge \frac{M_i}{\tau_i} \|\mathbf{d}_i - \mathbf{x}\|\}$$

Each pair of spacecraft define the line

$$\{\mathbf{x} \in \mathbb{R}^3 : \frac{M_j}{\tau_j} \|\mathbf{d}_j - \mathbf{x}\| = \frac{M_i}{\tau_i} \|\mathbf{d}_i - \mathbf{x}\|\,.$$

These lines form the boundaries of $\mathcal{D}_j$. Figure 5 shows a sequence of plots that describe how $\mathcal{D}_3$ is defined for a constellation of four spacecraft. Plots (a),

(b), and (c) define the regions corresponding to $\frac{M_3}{\tau_3}\|\mathbf{d}_3 - \mathbf{x}\| > \frac{M_1}{\tau_1}\|\mathbf{d}_4 - \mathbf{x}\|$, $\frac{M_3}{\tau_3}\|\mathbf{d}_3 - \mathbf{x}\| > \frac{M_2}{\tau_2}\|\mathbf{d}_2 - \mathbf{x}\|$, and $\frac{M_3}{\tau_3}\|\mathbf{d}_3 - \mathbf{x}\| > \frac{M_4}{\tau_4}\|\mathbf{d}_1 - \mathbf{x}\|$ respectively. Plot (d) defines the region $\mathcal{D}_3$ as the intersection of these three regions. In a similar manner, regions $\mathcal{D}_1$, $\mathcal{D}_2$, and $\mathcal{D}_4$ can be defined.

The following two lemmas ensure that for any configuration of N spacecraft, there are at most N disjoint regions that completely fill $\mathbb{R}^3$.

Lemma 1 $\mathcal{D}_i \cap \mathcal{D}_j = \emptyset, \quad i \neq j.$

Proof: See the appendix.

Lemma 2 $\cup_{i=1}^{N} \bar{\mathcal{D}}_i = \mathbb{R}^N.$

Proof: See the appendix.

The contours in Figure 4 (a) indicate that while J is not convex, it is continuous and has a unique minimum. The question is whether a gradient descent algorithm can be used to minimize J. The following theorem characterizes the continuity of J and its gradient.

Theorem 1 *If* $\sum_{\ell=1}^{N} f_\ell(t_f) \neq 0$, *then the following statements hold.*

1. $J(\mathbf{r}_R)$ *is continuous on* $\mathbb{R}^3$.
2. *If* $\frac{M_i}{\tau_i} = \frac{M_j}{\tau_j}$ *for all* $i, j \in 1, \ldots, N$, *then* $J(\mathbf{r}_R)$ *is continuously differentiable on* $\mathbb{R}^3$.
3. *Otherwise, it is continuously differentiable on* $\cup_{\ell=1}^{N} \mathcal{D}_\ell$ *(but not on the boundaries).*

Proof: See the appendix.

Optimization Procedure

All that remains is to choose an optimization algorithm that minimizes J in Equation (2) to find the fuel optimal center of rotation $\mathbf{r}_R$. Since gradient information is available, it is possible to use a gradient descent algorithm that is modified to handle the possible discontinuities between the regions $\mathcal{D}_\ell$. An alternative is to use a direct search method such as the Nelder-Mead Simplex method described in Ref. 14 and [15, pp. 305–309] . The advantage for this particular problem is that derivative information is not used, and the algorithm easily passes over the discontinuities in the gradient. Also, efficient implementations of the Nelder-Mead algorithm exist [16, pp. 2.4–2.5]. One of the disadvantages of the Nelder-Mead algorithm is that it can be very expensive and/or time-consuming for problems with objective functions that are severely elongated or when the dimensions of the problem become large.[14] Since Equation (2) does not suffer from either of these problems, it appears to be well suited for our application. The Nelder-Mead algorithm is initialized, by using the center of inverse fuel mass at time t_0, defined in Equation (17), and shown with an 'O' in Figure 4. The point $\mathbf{r}_R^{(0)}$ is seen to be relatively close to the desired minimum of J.

Based upon the constellation rotation trajectory determined by the optimization process, the open-loop control law for each of the ℓ spacecraft can

be found:

$$\mathbf{T}_\ell = M_\ell \mathbf{a}_\ell = M_\ell(\mathbf{a}_{r\ell} + \mathbf{a}_{t\ell})$$

$$= \begin{cases} M_\ell\left[\alpha\mathbf{z} \times \mathbf{r}_{R\ell} + (\alpha t)^2\mathbf{z} \times (\mathbf{z} \times \mathbf{r}_{R\ell})\right]; & 0 \le t \le t_w \\ M_\ell(\alpha t_w)^2\mathbf{z} \times (\mathbf{z} \times \mathbf{r}_{R\ell}); & t_w \le t \le t_f - t_w \cdot \\ M_\ell\left[-\alpha\mathbf{z} \times \mathbf{r}_R\ell + (\alpha(t_f - t))^2\mathbf{z} \times (\mathbf{z} \times \mathbf{r}_{R\ell})\right]; & t_f - t_w \le t \le t_f \end{cases} \tag{18}$$

The torque for $0 \le t \le t_w$ causes the formation to "spin-up," the torque for $t_w \le t \le t_f - t_w$ causes the formation to spin at a constant rate, and the torque for $t_f - t_w \le t \le t_f$ causes the formation to "spin-down."

Simulation Results

This section describes simulation results using the approach described in this paper. Simulations were performed in Matlab and Simulink. The numerical values used for the simulation are given in Table 1 with the exception that the mass distribution is changed to $M = (200, 200, 200, 200)$ (kg). The initial fuel distribution is $f_\ell(t_0) = (1, 1, 1, 1)$ (kg). The parameter μ allows tradeoffs between minimizing the total fuel used and equalizing fuel across the formation. When $\mu = 0$ fuel is minimized, as $\mu \to \infty$ fuel is equalized. The fuel used by each spacecraft after a single 90 degree rotation is shown in Figure 6. Figure 6 (a) is for $\mu = 0$ (i.e., fuel minimization), Figure 6 (b) is for $\mu = 100$ (i.e. a trade-off between fuel minimization and fuel equalization), and Figure 6 (c) is when $\mu = 10^5$ (i.e. fuel equalization). The total fuel used

by all the spacecraft is 0.0014 (kg) for $\mu = 0$, 0.0015 (kg) for $\mu = 100$, and 0.0016 (kg) for $\mu = 10^5$. Notice that when fuel is equalized, it is not necessarily minimized. In general, minimization and equalization are conflicting criteria.

The fuel used after 15 consecutive randomly selected rotations, is also shown in Figure 6. Cases where $\mu = 0$, $\mu = 100$ and $\mu = 10^5$ are shown in subplots (a), (b), and (c) respectively. For $\mu = 0$ the total fuel used was 0.0058 (kg), for $\mu = 100$ (kg) the total fuel used was 0.0107 (kg), for $\mu = 10^5$ the total fuel used was 0.0116 (kg).

Conclusions

The physical location of the axis about which a constellation of spacecraft rotates, determines the fuel consumed by each spacecraft during the maneuver. In this paper we have derived an algorithm that finds the optimal location for the axis of rotation, trading off overall fuel minimization and fuel equalization across a constellation of spacecraft in free space. The simulation results show that fuel minimization and fuel equalization are conflicting criteria. It is particularly important to note that minimum fuel rotations will result in fuel starvation for some spacecraft. Fuel is simultaneously minimized and equalized only if the spacecraft are an equal distance from the center of inverse fuel mass, and the thrust capabilities of the spacecraft are identical. This would be the case for three identical spacecraft in an equilateral triangle, but is not true if the spacecraft are not identical.

The control law derived in this paper defines fuel optimal trajectories for

each spacecraft in the constellation. These trajectories could be used for feedforward control, with additional feedback used for robustness to uncertainties and disturbance rejection. Since the approach taken is conservative (only the most performance-limited spacecraft is at its thrust limit at just two instants during the trajectory), the additional thrust required for feedback control could be easily accommodated by the spacecraft implying that the prescribed trajectories would still be feasible.

Finally, the optimization algorithm described in this paper could be used to determine the amount of fuel required by an entire interferometry mission. If the desired life of the mission, and the desired star locations are known, the amount of fuel required to transition between stars can be estimated with the algorithm described in this paper. This could be embedded in a larger optimization algorithm that computes the optimal sequence of stars, and the resulting fuel required for each spacecraft. If it is desired, for cost purposes, that the spacecraft be identical, then the optimization algorithm should be performed with large μ.

Acknowledgment

This work was performed in part at the Jet Propulsion Laboratory, California Institute of Technology under contract with the National Aeronautics and Space Administration. The research at BYU was supported by the Jet Propulsion Laboratory, California Institute of Technology under contract #96-1245. The authors thank the reviewers for their helpful comments.

References

[1] K. Lau, S. Lichten, L. Young, and B. Haines, "An innovative deep space application of GPS technology for formation flying spacecraft," in *American Institute of Aeronautics and Astronautics, Guidance, Navigation and Control Conference*, pp. 96–381, July 1996.

[2] T. M. Cover and J. A. Thomas, *Elements of Information Theory.* Wiley, 1991.

[3] P. K. C. Wang and F. Y. Hadaegh, "Coordination and control of multiple microspacecraft moving in formation," *The Journal of the Astronautical Sciences*, vol. 44, no. 3, pp. 315–355, 1996.

[4] P. Wang, F. Hadaegh, and K. Lau, "Synchronized formation rotation and attitude control of multiple free-flying spacecraft," *AIAA Journal of Guidance, Control and Dynamics*, vol. 22, pp. 28–35, January 1999.

[5] A. B. DeCou, "Orbital station-keeping for multiple spacecraft interferometry," *The Journal of the Astronautical Sciences*, vol. 39, pp. 283–297, July-Sept. 1991.

[6] C. R. McInnes, "Autonomous ring formation for a planar constellation of satellites," *Journal of Guidance, Control and Dynamics*, vol. 18, no. 5, pp. 1215–1217, 1995.

[7] Y. Ulybyshev, "Long-term formation keeping of satellite constellation using linear-quadratic controller," *Journal of Guidance, Control and Dynamics*, vol. 21, pp. 109–115, January-February 1998.

[8] R. Beard, R. Frost, and W. Stirling, "A hierarchical coordination scheme for satellite formation initialization," in *AIAA Guidance, Navigation and Control Conference*, (Boston, MA), pp. 677–685, August 1998. AIAA paper #98-4225.

[9] R. W. Beard and F. Y. Hadaegh, "Constellation templates: An approach to autonomous formation flying," in *World Automation Congress*, (Anchorage, Alaska), pp. 177.7–177.6, May 1998. ISIAC.

[10] R. W. Beard, T. W. McLain, and F. Y. Hadaegh, "Fuel equalized retargeting for separated spacecraft interferometry," in *American Control Conference*, (Philidelphia, PA), pp. 1580–1584, June 1998.

[11] R. W. Beard and F. Y. Hadaegh, "Fuel optimized rotation for satellite formations in free space," in *American Control Conference*, (San Diego, CA), pp. 2975–2979, June 1999.

[12] J. R. Wertz, ed., *Spacecraft Attitude Determination and Control.* Kluwer Academic Publishers, 1978.

[13] M. Athans and P. Falb, *Optimal Control.* New York, New York: McGraw-Hill Book Company, 1966.

[14] M. H. Wright, "Direct search methods: Once scorned, now respectable," in *Numerical Analysis* (D. F. Griffiths and G. A. Watson, eds.), Pitman Research Notes in Mathematics, pp. 191–208, Addison Wesley Longman Limited, 1995.

[15] W. H. Press, B. P. Flannery, S. A. Teukolsky, and W. T. Vetterling, *Numerical Recipes in C: The Art of Scientific Computing.* Cambridge University Press, 1988.

[16] The Math Works, Natick, Massachusetts, *Matlab Optimization Toolbox*, 1994.

Appendix

Proof of Lemma 1

Suppose that $x \in \mathcal{D}_i \cap \mathcal{D}_j$, then

$$x \in \mathcal{D}_i \implies \frac{M_i}{\tau_i} \|\mathbf{d}_i - \mathbf{x}\| > \frac{M_j}{\tau_j} \|\mathbf{d}_j - \mathbf{x}\|$$
$$x \in \mathcal{D}_j \implies \frac{M_j}{\tau_j} \|\mathbf{d}_j - \mathbf{x}\| > \frac{M_i}{\tau_i} \|\mathbf{d}_i - \mathbf{x}\|,$$

which is a contradiction.

Proof of Lemma 2

Pick an arbitrary $\mathbf{x} \in I\!R^3$. Suppose that $\mathbf{x} \notin \cup_{i=1}^{N} \bar{\mathcal{D}}_i$. $\mathbf{x} \notin \bar{\mathcal{D}}_1 \implies \frac{M_1}{\tau_1} \|\mathbf{d}_1 - \mathbf{x}\| < \frac{M_{\hat{j}}}{\tau_{\hat{j}}} \left\|\mathbf{d}_{\hat{j}} - \mathbf{x}\right\|$ for some $\hat{j} \in \{2, \ldots, N\}$. Re-number the spacecraft such that $\hat{j} = 2$, then $\frac{M_1}{\tau_1} \|\mathbf{d}_1 - \mathbf{x}\| < \frac{M_2}{\tau_2} \|\mathbf{d}_2 - \mathbf{x}\|$. $\mathbf{x} \notin \bar{\mathcal{D}}_2 \implies \frac{M_2}{\tau_2} \|\mathbf{d}_2 - \mathbf{x}\| < \frac{M_{\hat{j}}}{\tau_{\hat{j}}} \left\|\mathbf{d}_{\hat{j}} - \mathbf{x}\right\|$ for some $\hat{j} \in \{3, \ldots, N\}$. Re-number the spacecraft such that $\hat{j} = 3$, then $\frac{M_1}{\tau_1} \|\mathbf{d}_1 - \mathbf{x}\| < \frac{M_2}{\tau_2} \|\mathbf{d}_2 - \mathbf{x}\| < \frac{M_3}{\tau_3} \|\mathbf{d}_3 - \mathbf{x}\|$.

Repeat the argument for $\bar{\mathcal{D}}_3, \ldots \bar{\mathcal{D}}_{N-1}$ to get

$$\frac{M_1}{\tau_1} \|\mathbf{d}_1 - \mathbf{x}\| < \frac{M_2}{\tau_2} \|\mathbf{d}_2 - \mathbf{x}\| < \cdots < \frac{M_N}{\tau_N} \|\mathbf{d}_N - \mathbf{x}\| .$$

Now $\mathbf{x} \notin \bar{\mathcal{D}}_N \implies \frac{M_N}{\tau_N} \|\mathbf{d}_N - \mathbf{x}\| < \frac{M_{\hat{j}}}{\tau_{\hat{j}}} \left\|\mathbf{d}_{\hat{j}} - \mathbf{x}\right\|$ for some $\hat{j} \in \{1, \ldots, N-1\}$ which is a contradiction.

Proof of Theorem 1

Differentiating Equation (2) with respect to $\mathbf{r}_R$ gives

$$\frac{\partial J}{\partial \mathbf{r}_R} = \sum_{\ell=1}^{N} -2 \left(f_\ell(t_0) - f_\ell(t_f)\right) \frac{\partial f_\ell(t_f)}{\partial \mathbf{r}_R} + \sum_{\ell=1}^{N} \log\left(\frac{f_\ell(t_f)}{\sum_j f_j(t_f)}\right) \left[\frac{\left(\sum_j f_j(t_f)\right) \frac{\partial f_\ell(t_f)}{\partial \mathbf{r}_R} - f_\ell(t_f) \left(\sum_j \frac{\partial f_j(t_f)}{\partial \mathbf{r}_R}\right)}{\left(\sum_j f_j(t_f)\right)^2}\right].$$

Assuming that $\sum_j f_j(t_f) > 0$, then $\frac{\partial J}{\partial \mathbf{r}_R}$ is continuous if $f_i(t_f)$ and $\frac{\partial f_i(t_f)}{\partial \mathbf{r}_R}$ are continuous in $\mathbf{r}_R$. From Equations (16), (9), and (11) we obtain the following expression for $f_i(t_f)$:

$$f_i(t_f) = f_i(t_0) - \gamma M_i \|\mathbf{d}_i\| \left(\frac{2\hat{\phi}}{t_f(1-c)} + \frac{\hat{\phi}^2}{t_f(1-c)^2} - \frac{4\hat{\phi}^2 c}{3t_f(1-c)^2}\right).$$

Both c and $\|\mathbf{d}_i\|$ depend on $\mathbf{r}_R$ so

$$\frac{\partial f_i(t_f)}{\partial \mathbf{r}_R} = \frac{\partial f_i(t_f)}{\partial \|\mathbf{d}_i\|} \frac{\partial \|\mathbf{d}_i\|}{\partial \mathbf{r}_R} + \frac{\partial f_i(t_f)}{\partial c} \frac{\partial c}{\partial \mathbf{r}_R},$$

where

$$\frac{\partial f_i(t_f)}{\partial \|\mathbf{d}_i\|} = -\gamma M_i \left(\frac{2\hat{\phi}}{t_f(1-c)} + \frac{\hat{\phi}^2}{t_f(1-c)^2} - \frac{4\hat{\phi}^2 c}{t_f(1-c)^2} \right)$$

is a continuous function of $\|\mathbf{d}_i\|$ and

$$\frac{\partial f_i(t_f)}{\partial c} = -\gamma M_i \left(\frac{2\hat{\phi}}{t_f(1-c)^2} + \frac{2\hat{\phi}^2}{t_f(1-c)^3} - \frac{4\hat{\phi}^2(1+c)}{t_f(1-c)^3} \right),$$

is continuous in c as long as $c \in [0, \frac{1}{2}]$. $\|\mathbf{d}_i\| = \left\|(I - zz^T)(\mathbf{r}_i - \mathbf{r}_R)\right\|$ is clearly a continuously differentiable function of $\mathbf{r}_R$, so the continuity properties of J are determined by the continuity properties of c. c is a root of the sixth order polynomial given in Equation (12) which can be re-written in the following form which is standard for the Evans root locus:

$$1 + \frac{1}{K}\left[\frac{-(\hat{\phi}^4 + \hat{\phi}^2)c^2 + 2\hat{\phi}^2 c - \hat{\phi}^2}{c^6 - 4c^5 + 6c^4 - 4c^3 + c^2}\right] = 0.$$

By standard root locus theory, the roots are a continuous function of $\frac{1}{K} = \frac{\|\mathbf{d}_\beta\|^2 M_\beta^2}{\tau_\beta^2 t_f^4}$, where $\|\mathbf{d}_\beta\|$ and β are functions of $\mathbf{r}_R$. β is a constant function of $\mathbf{r}_R$ in each region $\mathcal{D}_j$, with a discontinuous switch on the boundaries. Therefore $1/K$ will also be a continuous function of $\mathbf{r}_R$ on each region, thereby establishing statement 3 of the lemma. At the boundaries $\|\mathbf{d}_\beta\|$ is continuous (but not differentiable) and so $1/K$ is continuous at the boundary if $\frac{M_i}{\tau_i} = \frac{M_j}{\tau_j}$ for all i, j, establishing statement 2. Since $\frac{\partial J}{\partial \mathbf{r}_R}$ is continuous for all but a set of measure zero (the region boundaries), J is continuous on all of $\mathbb{R}^3$.

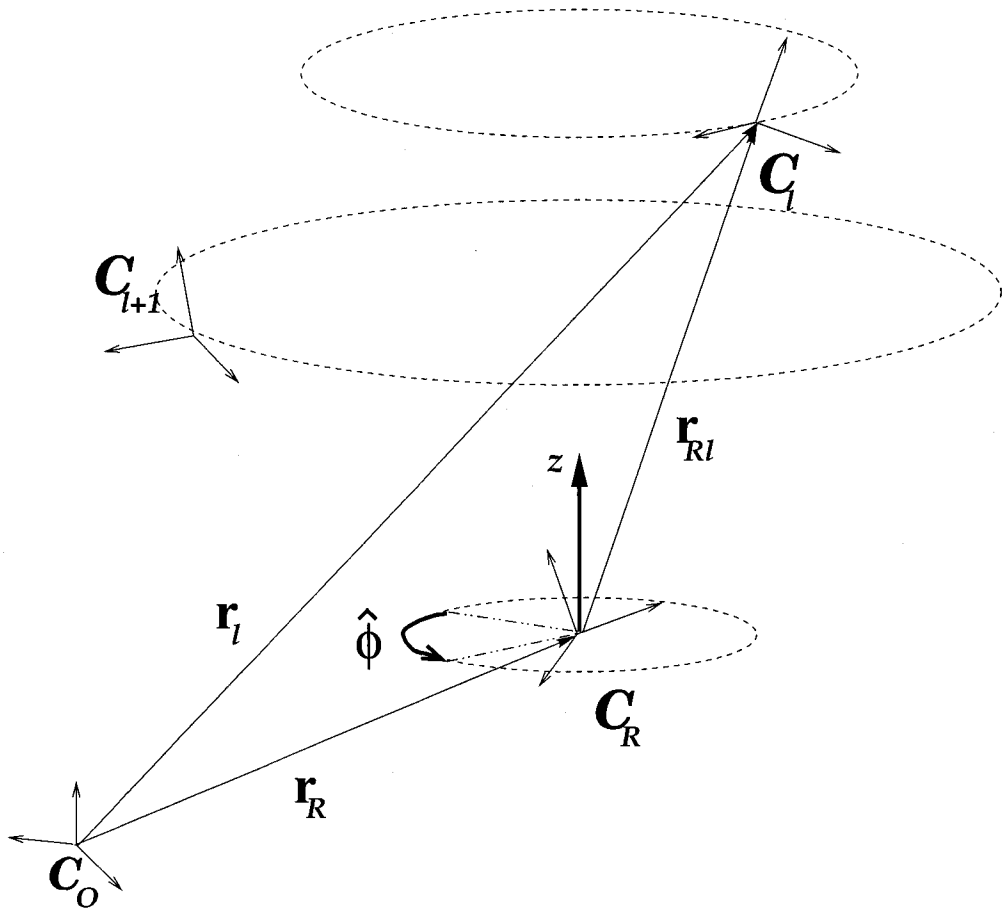

Figure 1: Problem Geometry

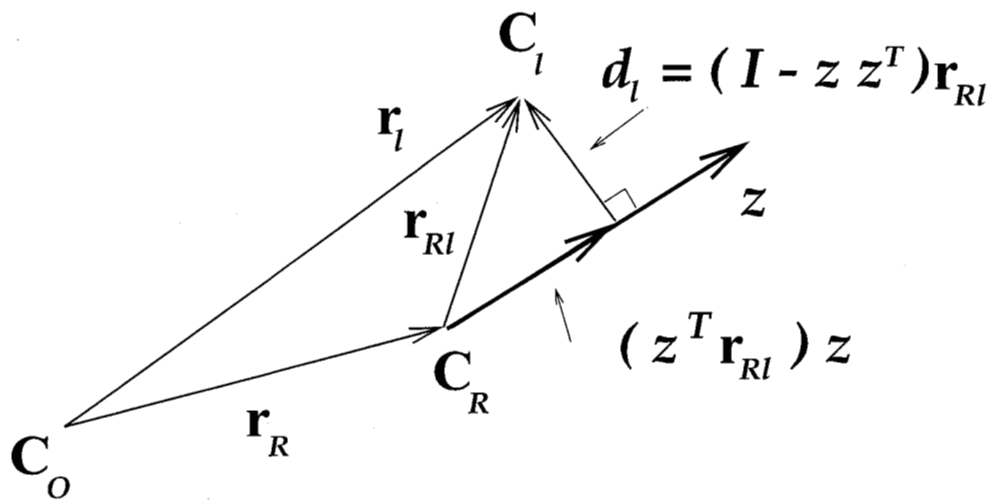

Figure 2: The distance of the ℓ^{th}spacecraft to the $\mathbf{z}$ axis.

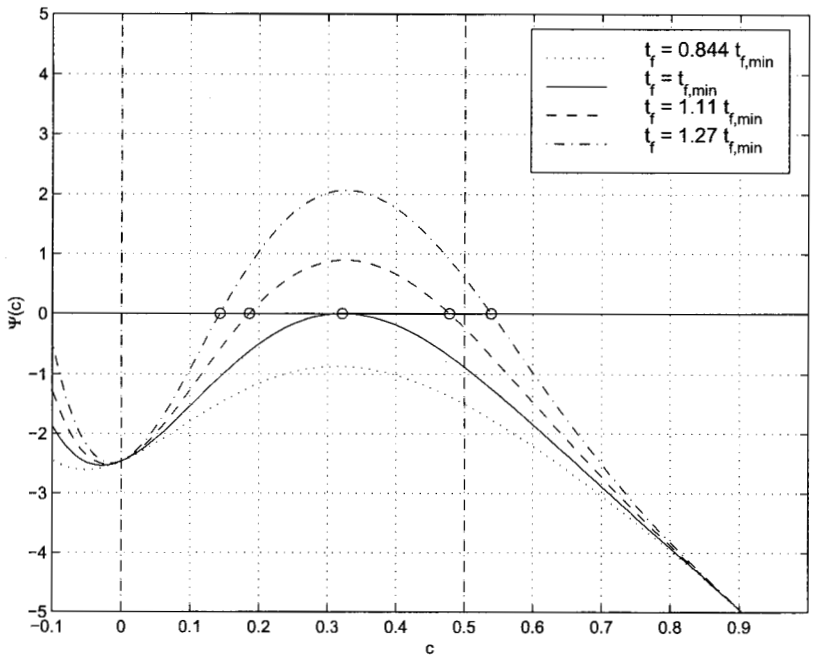

Figure 3: Roots of $\Psi(c)$.

$\mathbf{q}$	$(0, 0, \sin(\pi/2), \cos(\pi/2))^T$
$\mathbf{r}_1(t_0)$ (m)	$(110, 0, 0)^T$
$\mathbf{r}_2(t_0)$ (m)	$(0, 200, 0, 0)^T$
$\mathbf{r}_3(t_0)$ (m)	$(500, -500, 0)^T$
$\mathbf{r}_4(t_0)$ (m)	$(-100, -100, 0)^T$
τ (N)	$(700\mu, 700\mu, 700\mu, 700\mu)$
M (kg)	$(200, 100, 50, 200)$
t_f (sec)	40000
γ (sec/m)	0.000088673

Table 1: Parameters for Figure 4.

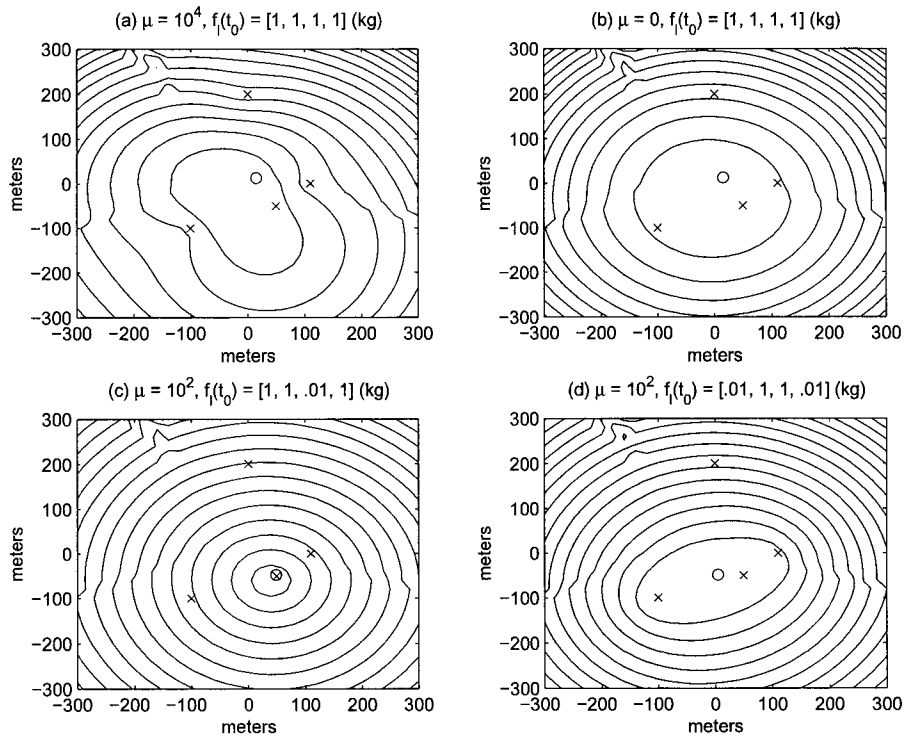

Figure 4: Contour plots of the function J.

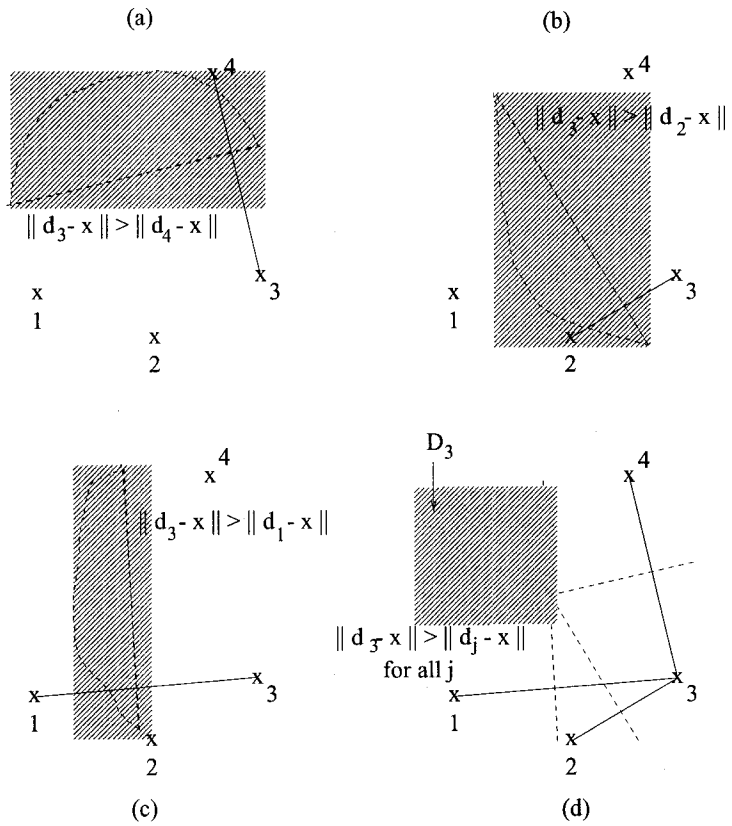

Figure 5: Defining region $\mathcal{D}_3$ for the objective function J.

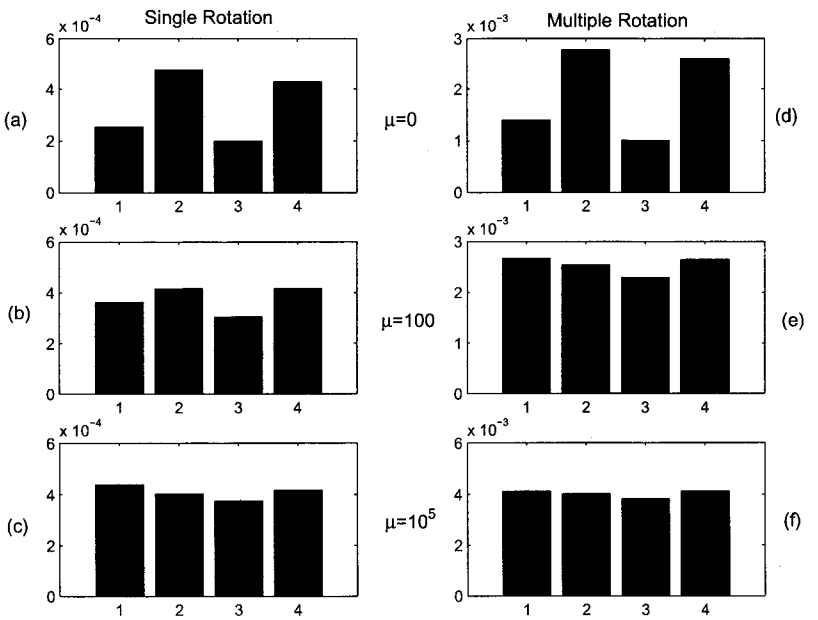

Figure 6: The fuel used after a single rotation.

Figure 1. Problem Geometry.

Figure 2. The distance of the ℓ^{th}spacecraft to the $\mathbf{z}$ axis.

Figure 3. Roots of $\Psi(c)$.

Figure 4. Contour plots of the function J.

Figure 5. Defining region $\mathcal{D}_3$ for the objective function J.

Figure 6. The fuel used after a single rotation.